A Smart Hyperthermia Nanofiber with Switchable Drug Release for Inducing Cancer Apoptosis

*Young-Jin Kim, Mitsuhiro Ebara, and Takao Aoyagi**

A smart hyperthermia nanofiber is described with simultaneous heat generation and drug release in response to 'on-off' switching of alternating magnetic field (AMF) for induction of skin cancer apoptosis. The nanofiber is composed of a chemically-crosslinkable temperature-responsive polymer with an anticancer drug (doxorubicin; DOX) and magnetic nanoparticles (MNPs), which serve as a trigger of drug release and a source of heat, respectively. By chemical crosslinking, the nanofiber mesh shows switchable changes in the swelling ratio in response to alternating 'on-off' switches of AMF because the self-generated heat from the incorporated MNPs induces the deswelling of polymer networks in the nanofiber. Correspondingly, the 'on-off' release of DOX from the nanofibers is observed in response to AMF. The 70% of human melanoma cells died in only 5 min application of AMF in the presence of the MNPs and DOX incorporated nanofibers by double effects of heat and drug. Taken together these advantages on both the nano- and macroscopic scale of nanofibers demonstrate that the dynamically and reversibly tunable structures have the potential to be utilized as a manipulative hyperthermia material as well as a switchable drug release platform by simple switching an AMF 'on' and 'off'.

1. Introduction

During the past few years increased attention has been given to stimuli-responsive or smart polymeric nanofibers owing to their ability to act as an 'on-off' reversible switch.[1] Their structures are uniquely advantageous because the nano-scale features provide extremely large surface area and porosity,[2] which enhance the sensitivity to external stimuli, while the macroscopic features enable facile manipulation as a bulk matter. In addition, polymeric nanofibers can be manufactured at a low cost in large quantities.[3] Indeed, polymeric nanofibers have already been utilized in the clinical field as wound dressings and anti-adhesive membranes.[4,5] Taken together these advantages on both nano- and macroscopic scales demonstrate that dynamically and reversibly tunable structures of smart nanofibers have the potential to be utilized for 'on-off' delivery of drugs or cells.[1c,d] Since smart polymers respond to small changes in external stimuli with large discontinuous changes in their physical properties,[6] the incorporation of a further functionality such as heat generation properties into smart nanofibers opens novel opportunities in biomedical fields such as hyperthermic therapy and beyond.

Magnetic nanoparticles (MNPs) have emerged as a key material for nanomedicines and shown huge potential in many biomedical applications, such as diagnosis, imaging and hyperthermia.[7] Among them, magnetic hyperthermia has been particularly attractive owing to its unique heat generation property when an alternating magnetic field (AMF) is applied to them. The magnetic hyperthermia, a type of cancer treatment in which body tissue is exposed to temperature higher than normal body temperature; ≈45 °C,[8] has been developed in the past decades as an efficacious treatment modality for localized or deeply exist cancer.[9] Magnetic hyperthermia has been also utilized in combination with chemotherapy to improve cancer cell therapy with anticancer drugs, since hyperthermia can render tumor cells temporarily more sensitive to the damaging effects of chemotherapeutics.[10] Due to difficulties in limiting delivering anticancer drugs or heat to the tumor region, MNPs in various forms such as hydrogels,[11a] spheres,[11b] liposomes,[11c] and micelles[11d] have been also developed to eradicate tumor cells by magnetic induction hyperthermia. When addressing the *in vivo* application of MNPs, however, the nano-dimensional properties can potentially lead to toxic side effects such as impaired mitochondrial function,[12a] inflammation,[12b,c] and DNA damage.[12d] From these perspectives, incorporation of MNPs into nanofibers for possible treatment of malignant epithelial tumors has become an area of interest because the nanofibers can be manipulated as a bulk material and utilized as an adhesive bandage while maintaining the nanoscale structures.

In this study, we develop smart hyperthermia nanofibers with both heat-generating and drug releasing abilities for improved hyperthermic chemotherapy. The hyperthermia nanofibers are developed by electrospinning temperature-responsive polymer

Y.-J. Kim, Prof. T. Aoyagi
Materials and Science Engineering
Graduate School of Pure and Applied Science
University of Tsukuba
1-1-1 Tennodai, Tsukuba, Ibaraki 305-8577, Japan
E-mail: AOYAGI.Takao@nims.go.jp
Y.-J. Kim, Dr. M. Ebara, Prof. T. Aoyagi
Biomaterials Unit
International Center for Materials Nanoarchitectonics (WPI-MANA)
National Institute for Materials Science (NIMS)
1-1 Namiki, Tsukuba, Ibaraki 305-0044, Japan

DOI: 10.1002/adfm.201300746

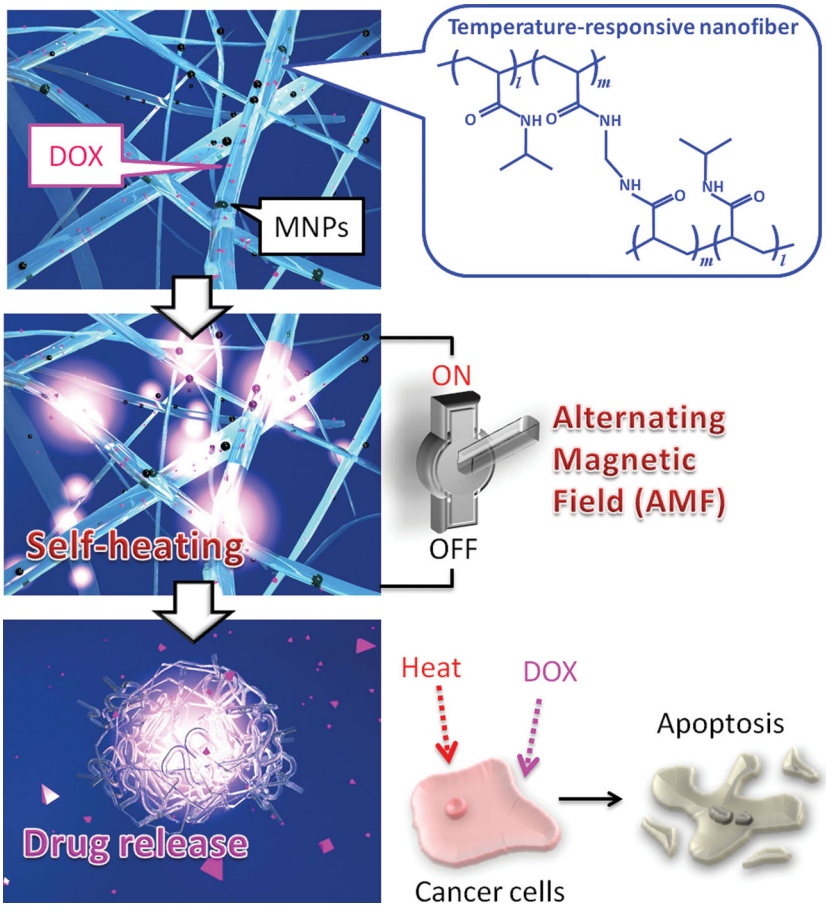

Figure 1. Design concept for a smart hyperthermia nanofiber system that utilizes MNPs dispersed in temperature-responsive polymers. Anticancer drug, doxorubicin (DOX), is also incorporated into the nanofibers. The nanofibers are chemically crosslinked. First, the device signal (AMF) is turned 'on' to activate the MNPs in the nanofibers. Then, the MNPs generate heat to collapse the polymer networks in the nanofiber, allowing the 'on-off' release of DOX. Both the generated heat and released DOX induce apoptosis of cancer cells by hyperthermic and chemotherapeutic effects, respectively.

blended with MNPs and anti-cancer drug (doxorubicin; DOX). Temperature-responsive polymers and MNPs serve as a trigger of drug release and a source of heat, respectively. Electrospinning is applicable to almost any soluble or fusible polymers and allows for the production of a variety of continuous fibers with uniform diameters ranging from micro- to nanometer scale.[13] However, one of the major challenges in the development of reversibly responsive smart nanofibers is the stability of water soluble polymers in aqueous media both above and below the lower critical solution temperature (LCST). For example, electrospun nanofibers from the *N*-isopropylacrylamide (NIPAAm) homopolymer are not stable in water and disperse easily.[1c,d] Therefore, copolymerization with crosslinkable monomers is required to obtain stable nanofibers in an aqueous medium with high sensitivity to temperature changes.[1c,d] Although physical crosslinking can be also accomplished by ionic or hydrophobic interactions,[14] the resulting bonding is thermally and mechanically unstable.[15] With this background, we have previously achieved the chemical crosslinking of NIPAAm-based nanofibers using thermal- or photo- crosslinkable co-monomers.[1c,d]

Here, we employ the thermal curable nanofiber which is fabricated by electrospinning copolymer of NIPAAm and *N*-hydroxymethylacrylamide (HMAAm) (poly(NIPAAm-*co*-HMAAm)). The methylol group in HMAAm is crosslinked by self-condensation under high temperature. The thermally crosslinked, MNP/DOX incorporated nanofibers demonstrate the switchable changes in the swelling ratio in response to alternating 'on-off' switches of AMF because the self-generated heat from the MNPs induced the deswelling of polymer networks. Finally, we demonstrate the ability to induce apoptosis in human melanoma cells of the smart hyperthermia nanofiber in vitro (**Figure 1**).

2. Results and Discussion

2.1. Fabrication of Temperature-Responsive Nanofibers and Thermally-Induced Crosslinking

Poly(NIPAAm-*co*-HMAAm) was copolymerized by free-radical polymerization with 80 and 20 mol% of NIPAAm and HMAAm in feed ratio, respectively (see Scheme S1a in the Supporting Information). The HMAAm content in the copolymer was determined by ^{1}H-NMR to be 19.4 mol% (Figure S1 in the Supporting Information), and the molecular weight (Mn) and polydispersity index (PDI) were estimated by GPC to be 14 kDa and 1.8, respectively. In general, lower molecular weight (<10 kDa) has been resulted in the formation of beads or particles instead of fine uniformed nano-/micro-sized fibers probably owing to insufficient molecular chain entanglement to retain molecular interaction to form a fiber from polymer solution jets. As the molecular weight increases, the fiber morphologies change beads form to fine fibers with thicker diameter.[16] Furthermore, the narrow PDI can contribute to the uniform nanofiber formation due to the molecular chain entanglements during electrospinning. Through the introduction of HMAAm units, the LCST of the copolymer can be adjusted to be near the hyperthermia temperature. Figure S2 (Supporting Information) shows the LCST of the copolymer (approximately 48 °C). The LCST was set above 45 °C because it decreases a few degrees after self-condensation (crosslinking) of hydrophilic methylol groups.

The thermally-crosslinkable and temperature-responsive nanofiber was fabricated by electrospinning with optimized conditions (**Figure 2**a). Briefly, the poly(NIPAAm-*co*-HMAAm) solution was prepared by dissolving the copolymer in HFIP at 15 w/v%. As shown in Figure 2b, nanofibers were randomly distributed to form the continuous fibrous structure with an average diameter of 350 nm without beads or particles. During the electrospinning, high volatility organic solvent, that could

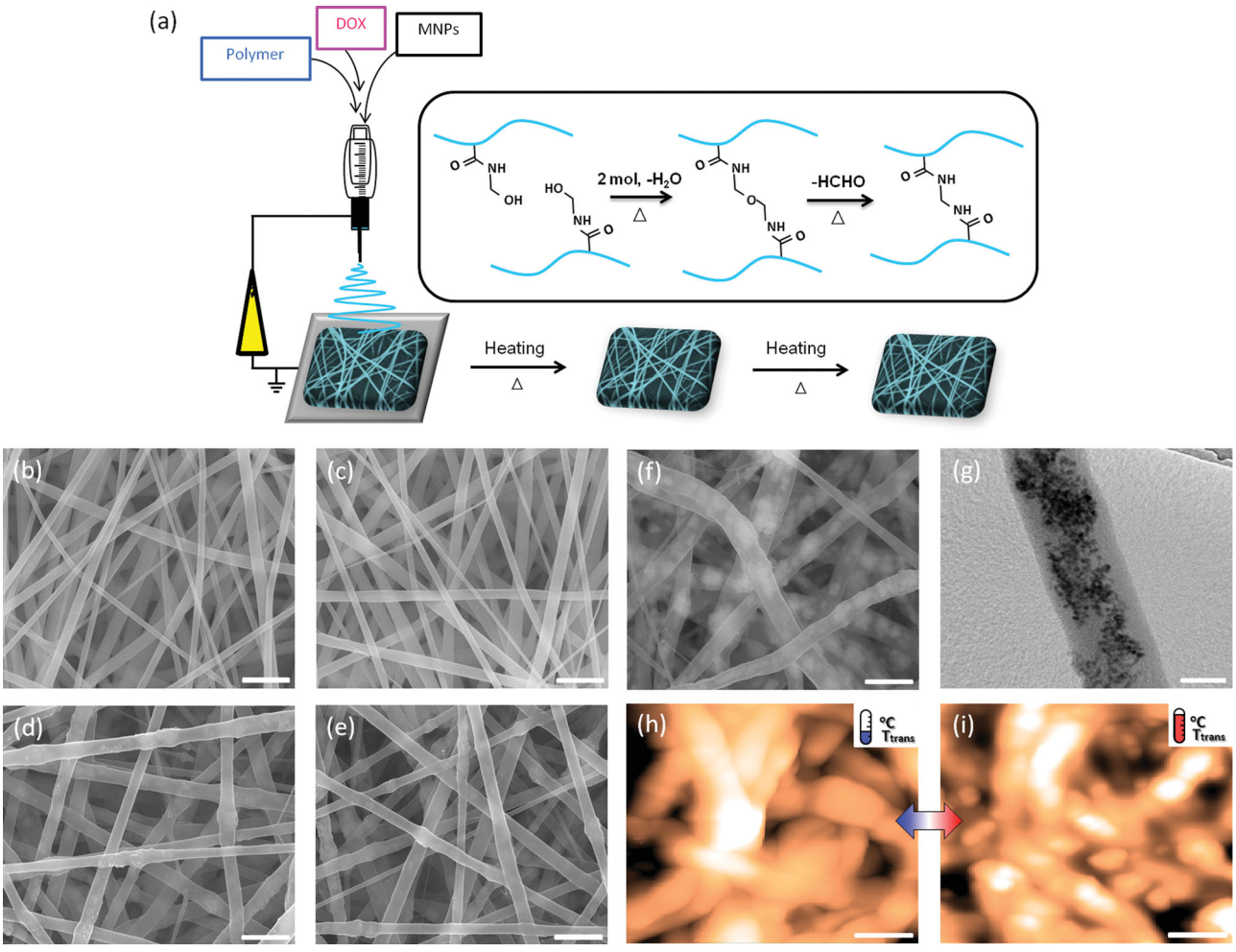

Figure 2. a) Preparation of thermally-crosslinkable temperature-responsive nanofibers by electrospinning and thermal curing processes by self-condensation. SEM images of electrospun poly(NIPAAm-*co*-HMAAm) b) before and c) after thermal crosslinking (scale bars are 2 μm), and DOX/MNPs-nanofibers (31 wt% of MNPs in feed and 0.18 wt% of DOX in feed) d) before and e) after crosslinking (scale bars are 1 μm). f) SEM (BSE mode) image and g) TEM image of the MNPs-nanofibers with 31 wt% of MNPs after thermal curing (scale bars are 1 μm (SEM) and 200 nm (TEM), respectively). The AFM images of crosslinked MNPs-nanofibers with 31 wt% of MNPs after water treatment at h) 20 °C and i) 50 °C (scale bars are 1 μm).

be harmful to cells or tissues in biomedical applications, was evaporated and residual solvent was completely removed using higher vapour pressure oven.[17] The chemically intermolecular crosslinking of the electrospun nanofiber was carried out by thermal curing of the methylol groups in HMAAm (Figure 2a). The two methylol groups are immediately formed a bis(methylene ether) by self-condensation reaction under high temperature (>100 °C). By further continuous heating, the bis(methylene ether) is transformed into a very stable methylene bridge simultaneously with evaporation of a formaldehyde molecule (see Scheme S1b in the Supporting Information). The morphologies of the nanofibers after thermal curing were observed by scanning electron microscope (SEM). Even after thermal curing, the morphology and diameter were preserved (Figure 2c). Successful intermolecular crosslinking was quantitatively determined from the disappearance of the peaks corresponding to methylol groups in the ATR-FTR spectra of the nanofibers according to a previously published method.[1c] Approximately 50% of the methylol groups was involved in the crosslinking process (data not shown). Fibrous structures are still visible in the crosslinked nanofibers in an aqueous solution both below and above LCST.

2.2. DOX and MNPs-embedded Hyperthermia Nanofibers

DOX and MNPs-embedded hyperthermia nanofiber was also fabricated by electrospinning. In general, there are many limitations to prepare composite nanofibers by electrospinning due to the needle clogging, poor dispersion of additives, or negative effect on spinnability.[18] In this study, therefore, positively charged MNPs were used because they show a good dispersion in both organic and aqueous media due to the charge repulsion between nanoparticles. In addition, we employed a mixture of magnetite (Fe_3O_4) and maghemite (γ-Fe_2O_3) MNPs in this study because magnetite alone is not stable in oxidation,

acid/base solvents, and wide range of temperature.[19] We have chosen HFIP as a solvent for electrospinning because use of HFIP generally results in good spinnability and reproducibility even for a variety of polymer solution.[20] MNPs and DOX were first dispersed in distilled water with concentrations of 0.1–0.2 g and 1 mg in 300 µL of distilled water, respectively. The DOX/MNPs solution was then mixed with poly(NIPAAm-*co*-HMAAm) solution (15 w/v% in HFIP) in a 10/1 volume ratio to obtain 18–31 wt% and 0.18 wt% of the final weight fractions of MNPs and DOX in the polymer, respectively. The electrospun nanofibers were subsequently crosslinked by self-condensation of the methylol group of HMAAm upon heating. The morphologies of the MNP/DOX-incorporated nanofibers before and after thermal curing were observed by SEM (Figure 2d,e). The nanofibers were randomly distributed to form the continuous fibrous structure and incorporation of MNPs and DOX did not alter the structure. The morphology and diameter were preserved even after thermal crosslinking. Moreover, both high voltage SEM (back-scattered electrons; BSE) and transmittance electron microscope (TEM) images reveal that the MNPs were successfully incorporated within the fiber (Figure 2f,g). To test the stability in solution of the crosslinked nanofibers, they were immersed in phosphate buffered saline (PBS) and equilibrated at 20 and 50 °C (below and above the LCST). The morphologies were examined by atomic force microscope (AFM) under wet conditions after removing the excess water. AFM images indicate that the crosslinked nanofibers did not dissolve in water and the fibrous structures are still visible both below and above the LCST (Figure 2h,i). In contrast, the non-crosslinked nanofibers were completely dissolved within 30 seconds in PBS below the LCST and the incorporated MNPs aggregated.

To determine the amount of embedded MNPs in nanofibers, thermogravimetric analysis (TGA) was employed. Figure S3 (Supporting Information) shows the weight loss of the nanofibers when heated to 600 °C. From the non-volatilized fraction, the embedded MNPs in the fibers were estimated to be 15 and 24 wt% for 18 and 31 wt% in feed, respectively. This may be because the concentration of the MNPs in the starting solution and the resulting fibers was not the same due to electrospinning processing. We also performed energy dispersive X-ray spectroscopy (EDX). The result revealed that the embedded MNPs were 11 and 22 wt% for 18 and 31 wt% in feed, respectively (Table S1 in the Supporting Information). This could be explained by the limitation of EDX measurement that characterizes only surface nearby while TGA characterizes a whole material. The X-ray diffraction (XRD) patterns of the MNPs in the fibers were shown in Figure S4 (Supporting Information). The diffraction peaks appeared at 2θ = 40.14, 35.44, 43.04, 53.5, 57.02, 62.74 and 74.29°, which are the characteristic peaks of MNPs crystals.

2.3. Magnetic and Heat Generation Properties of Nanofibers

To investigate the response of the nanofibers to a magnetic field, a neodymium magnet was kept near a dish (10 cm in diameter) in which MNPs-nanofiber floats (**Figure 3**a). The

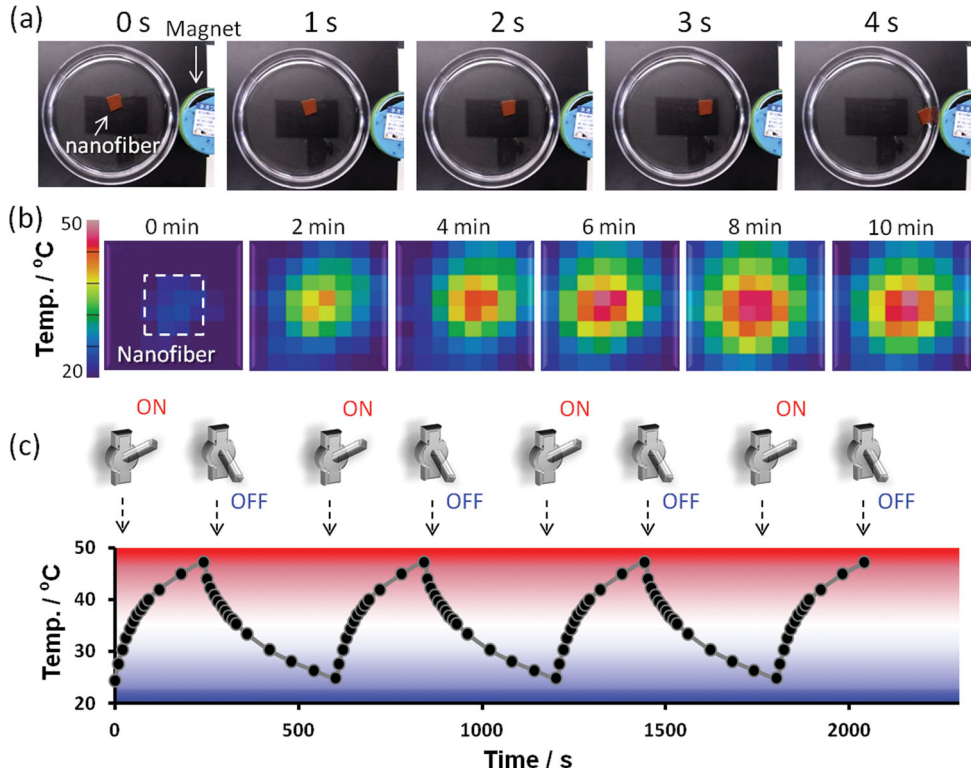

Figure 3. a) Magnet-responsive behaviour of crosslinked DOX/MNPs-nanofiber. A neodymium magnet was kept near a water-floated nanofiber. b) Time-dependent infrared thermal images of the DOX/MNPs-nanofiber in an AMF. c) Heating and cooling profile of the DOX/MNPs-nanofiber in response to alternating switching of AMF.

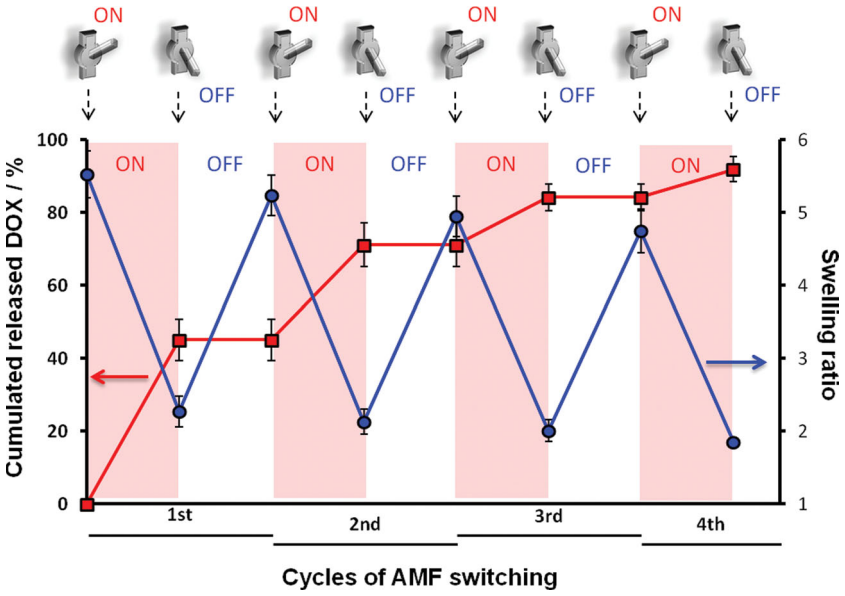

Figure 4. 'On-off' switchable and reversible heat profile and swelling ratio of crosslinked MNPs-nanofibers with increasing 'on-off' switching cycle of AMF, and DOX release profile corresponding to reversible swell-shrink property in response to temperature changes. DOX release = $D_{released\ at\ X}$/ $D_{total} \times 100$ (%), where $M_{released\ at\ X}$ is the cumulative amounts of released DOX at X cycle of AMF alternation and M_{total} is the total amounts of incorporated DOX in MNPs-loaded nanofiber. Swelling ratio = $(W_{swell} - W_{dry})/ W_{dry}$, where W_{swell} is weight of swelled MNPs-loaded nanofiber and W_{dry} is weight of dried MNPs-nanofiber.

MNPs-nanofiber was quickly attracted by the magnet within 5 s. This magnetic field-responsive behaviour enables remote manipulation of nanofiber under a controlled magnetic field. The heat generation property of the MNPs-nanofibers in an AMF was also evaluated. Ferromagnetic magnetite particles have an AMF-induced heating ability and generate heat in an AMF because of magnetic hysteresis loss.[21] Figure S5 (Supporting Information) shows the time-dependent heating of the nanofiber with different MNP compositions in an AMF with 480 A. For the nanofiber with 18 wt% MNP without crosslinking, the temperature increased from 4 °C to 29, 41 and 51 °C after 600 seconds for nanofibers with contents of 5, 15 and 25 mg of the sample weight in 300 µL of PBS, respectively (Figure S5a). For 31 wt% MNP nanofiber without crosslinking, the temperature increased to 29, 44 and 72 °C after 600 s for nanofibers with contents of 5, 15 and 25 mg of sample weight in 300 µL of PBS, respectively (Figure S5b). Therefore, the heat generation property of MNPs clearly depends on their concentrations and total amounts. After crosslinking, however, the heating ability of 31 wt% MNP nanofibers decreased (the temperature increased to 26, 32 and 44 °C after 600 s for nanofibers with contents of 5, 15 and 25 mg of sample weight, respectively) (Figure S5c). The possible explanation is that for the nanofiber without crosslinking, the incorporated MNPs were easily dispersed from the nanofibers upon heating and the released MNPs aggregated to form a large aggregate. Consequently those aggregates may contribute to the enhanced temperature increasing in the initial step of AMF application (Supporting Information Figure S5).[22] This result also indicates that crosslinking process is very important for reduction of side effects of eluted MNPs.[23]

Figure 3b shows the infrared thermal images of nanofiber (25 mg/ 300 µL, after crosslinking) with 31 wt% of MNP in an AMF application. A temperature increase is observed in the center of images where the nanofiber was located. Moreover, 'on-off' heat generation property is monitored in response to alternating 'on' and 'off' switching of AMF (Figure 3c). These results indicate that the MNPs-nanofiber has the potential to be used for hyperthermia treatment. On the basis of these results, this composition (MNPs; 31 wt%, sample; 25 mg) was selected for further study.

2.4. 'On-Off' Switchable Drug Release

Next, we demonstrate the switchable changes in the swelling ratio and the corresponding drug release in response to alternating 'on-off' switches of AMF. **Figure 4** shows the changes in the equilibrium swelling ratio of the DOX/MNPs-nanofiber and the corresponding result of drug release from the same nanofibers in response to 'on' and 'off' switching of AMF application. Because poly(NIPAAm-*co*-HMAAm) is soluble in aqueous media below LCST and dehydrates sharply as temperature is raised above the LCST, the crosslinked poly(NIPAAm-*co*-HMAAm) nanofibers reversible changes in the swelling ratio in response to temperature changes. The DOX/MNPs-nanofibers were first swelled at 25 °C in PBS for 10 min. Next, the AMF was turned 'on' for 300 s allowing the MNPs-nanofiber to heat to 45 °C. The AMF was then turned 'off' for another 300 s allowing cooling them down to 25 °C. This process was repeated 4 times. The swelling ratio was found to change reversibly recovered within each cycle. Correspondingly, the 'on-off' release of DOX from the nanofiber was observed in response to temperature changes. The incorporated drug is released by it being squeezed out of the collapsing polymer network above the LCST. In the our previous study, we have successfully demonstrated the 'on-off' switchable release of drugs from temperature-responsive nanofibers.[1c] Approximately 45, 26, 13, and 7% of the loaded DOX were released in the 1st, 2nd, 3rd, and 4th cycles of AMF application, respectively. In other words, almost all of the DOX (> 90%) was released after 4 cycles, whereas only negligible amounts of DOX were released during the cooling 'off' process. These results indicate that non-specific interactions between the nanofibers and DOX maintained DOX within the nanofiber interior at 'off' state. At 'on' state, on the other hand, the nanofibers deswelled and deformed, triggering the release of the drug molecules. In general, the application of bulk materials such as hydrogels for drug delivery system is limited by their slow response.[24a] Therefore, much effort has been made to increase the rate of response, such as reducing the size or constructing an interconnected pore structure within the gel.[24b,c] Because of the high specific surface area of nanofibers, they are more sensitive to small changes in external stimuli than corresponding bulk materials. Thereby, we

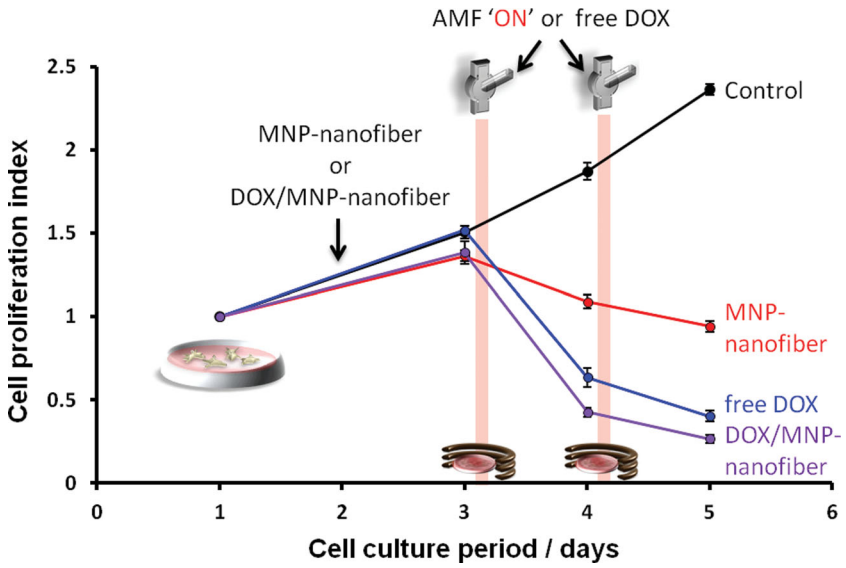

Figure 5. In vitro anticancer tests involving the DOX/MNPs-nanofibers and human melanoma (COLO 679) cells. The effect of AMF treatment on the proliferation of cells determined by an MTT assay. The cells were cultured at 37 °C for 2 days. MNPs-nanofiber (red line) or DOX/MNPs-nanofiber (purple line) was then added to the medium and cells were co-incubated at 37 °C for another 24 h. AMF was then turned 'on' for 5 min to increase the medium temperature to 45 °C at day 3 and day 4. Cells were also incubated in the absence of nanofibers with (blue line) and without (black line) free DOX addition at day 3 and day 4. Proliferation index = $N_D/N_{D=1}$, where N_D = cell number on day D, $N_{D=1}$ = cell number on day 1.

took advantage of the nano sized effects of nanofibers for the 'on-off' switchable release of drug. In addition, the proposed AMF system allows the control of switchable drug release by simply switching the AMF 'on' and 'off'.

2.5. Anticancer Effects

Recently, many approaches for hyperthermic cancer cell therapy have been pursued using hybrid nanoarchitectures with MNPs.[8a,23a,25] However, those hybrids cannot be directly used in conjunction with living matter because nano-dimensional properties can potentially lead to toxic side effects. Moreover, both the DOX and hyperthermia can induce apoptosis in not only cancer cells but also normal cells.[26] One of the advantages of this system is that a nanofiber can be manipulated as a bandage or compress. In other words, the nanofiber can be transplanted directly to the tumor region during surgery. From this regard, in this study, MNPs were stably incorporated within the crosslinked nanofibers for possible treatment of malignant epithelial tumors by both hyperthermia and chemotherapeutic effects. To test both hyperthermia and chemotherapeutic effects of the DOX/MNPs-nanofiber in vitro, the cytotoxicity of human melanoma cell line COLO 679 cells were evaluated by MTT assay for 1, 3, 4 and 5 days. The cancer cells (1.0×10^4 cells/well) were cultured at 37 °C for 2 days. MNPs-nanofiber or DOX/MNPs-nanofiber was then added to the cell cultured wells for co-cultivation with nanofibers and cells were further incubated for 24 h at 37 °C (**Figure 5**). It can be noted that, compared with the control (medium only), there were no significant decreases in the proliferation index of the cells in the presence of MNPs-nanofibers and DOX/MNPs-nanofibers. This result indicates that both DOX and MNPs were stably incorporated in the nanofiber matrices and were not released without AMF application ('off' state). This result corresponds well to the in vitro drug release study (Figure 4). On testing the hyperthermia effect on the cells, an AMF was then turned 'on' at day 3. The temperature of the medium was increased to 45 ± 1 °C and then maintained for up to 5 min. This treatment was repeated again at day 4. The cell viability decreased about 20% in the presence of MNPs-nanofiber without DOX in a magnetic field for 5 min duration. Although the cancer cell killing effect was still low (approximately 80% of cells were survived), the magnetic field induced hyperthermia successfully affects cell viability over a period of 5 min. This can be improved as the time of the hyperthermia treatment is increased. In case of the DOX/MNPs-nanofiber, on the other hand, cell viability decreased to 70% by AMF application. Although the hyperthermia effect itself showed a minor anticancer effect for a short duration AMF application, DOX released from the nanofibers induced the apoptosis of cancer cells due to a synergistic effect in combination with hyperthermia.[27] Indeed, more cells were killed by double effect of DOX/MNPs-nanofiber than by chemotherapeutic effect of free DOX treatment, even though the total amount of released DOX from DOX/MNP-nanofiber was almost similar to that of free DOX. This result indicates that the proposed drug release system is more advantageous to conventional chemotherapy because no inherent cytotoxicity was detected for the DOX/MNP-nanofibers without external AMF application.

Since hyperthermia can kill cancer cells by a number of pathways, including apoptosis, the viability of the cells was also demonstrated by fluorescent staining with annexin V Cy-3 and terminal deoxynucleotidyl transferase-mediated dUTP nick end labelling (TUNEL) assay.[28] In general, apoptosis initially induces the inversion of phosphatidylserin, which allows binding to annexin V. Therefore, annexin V detects an early stage apoptosis while TUNEL assay detect the late stage apoptosis.[29] For MNPs-nanofiber, only annexin V stained cells were detected, indicating that the cause of cell death is primarily membrane rapture. For DOX/MNPs-nanofiber and free DOX, although TUNEL stained cells were not observed at day 4 (Figure S6 in the Supporting Information), both annexin V and TUNEL stained cells were observed at day 5, indicating late-stage apoptosis (**Figure 6**). These results indicate that the double effect of DOX treatment and hyperthermia effectively induced apoptosis while the effect of a single hyperthermia on apoptosis was not significant for a short time AMF treatment.

3. Conclusions

In summary, this study demonstrated dynamically and reversibly switchable behaviour of smart hyperthermia nanofibers in

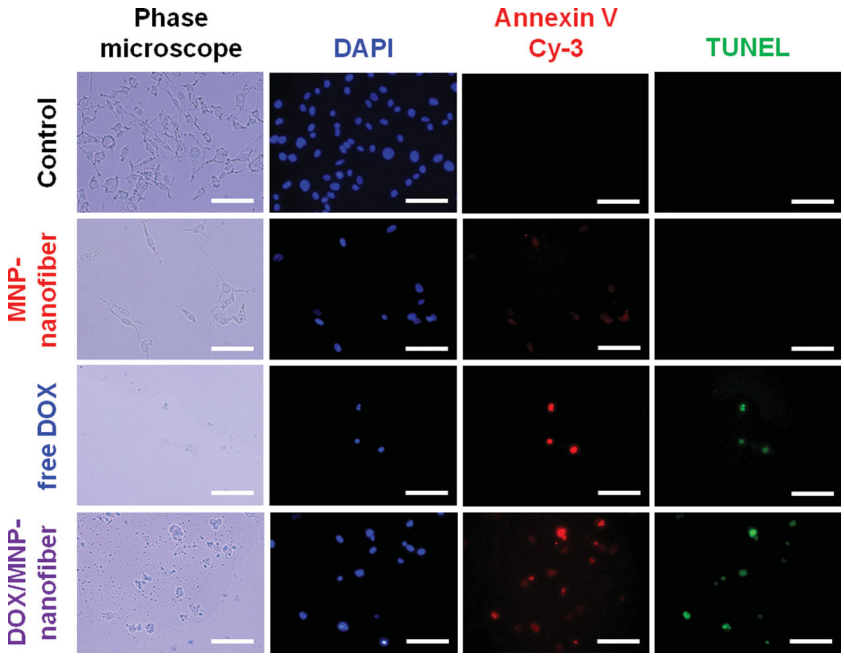

Figure 6. Fluorescence images demonstrating the cell death pathway by DAPI (blue), annexin V (red), and TUNEL (green) staining after cultivation of 5 days (scale bars are 100 μm).

response to the self-generated heat from the incorporated MNPs in the smart nanofiber upon the magnetic field application. The smart hyperthermia nanofibers were fabricated by an electrospinning method with a thermally curable temperature-responsive polymer, MNPs, and DOX. By chemical crosslinking, the nanofibers showed the quick and reversible changes in the swelling ratio in response to alternating 'on' and 'off' switches of AMF application and, the resulting 'on-off' drug release from the fibers was observed. The DOX/MNPs-nanofiber induced the apoptosis of cancer cells due to a synergistic effect of chemotherapy and hyperthermia. Taken together these advantages on both the nano-dimensional drug release and macro-dimensional hyperthermic effect of smart nanofibers demonstrate that the dynamically and reversibly tunable structures of smart nanofibers have the potential to be utilized as a manipulative hyperthermia material as well as a switchable drug release platform by simple switching an AMF 'on' and 'off'.

4. Experimental Section

Synthesis and Characterization of Thermally Crosslinkable Temperature-Responsive Polymers: *N*-Isopropylacrylamide (NIPAAm) (Kojin, Japan) and *N*-hydroxymethylacrylamide (HMAAm) (TCI, Japan) were copolymerized as described previously (Scheme S1 in the Supporting Information).[1c,30] Briefly, NIPAAm (80 mol%), HMAAm (20 mol%) and 2,2′-azobis(isobutyronitrile) (AIBN, 0.01 mol% of total monomer concentration) (Wako, Japan) were dissolved in *N,N*-dimethylformamide (DMF, 20 mL) (Wako, Japan). A total monomer molar concentration was 50 mmol. The copolymerization was carried out at 62 °C for 20 h after completely degassed by four times of freezing and thawing cycles. After the polymerization, AIBN, unreacted monomers, impurities and solvent were removed by dialysis against ethanol and distilled water for seven days. The dialyzed solutions were lyophilized for four days. The chemical structure of the obtained copolymer was confirmed by ^{1}H-NMR (JEOL, Japan). The number of molecular weight (Mn) and polydispersity index (PDI) of the copolymer were determined by gel permeation chromatography (GPC, JASCO International, Japan) using DMF with lithium bromide (LiBr, 10 mM) as an eluent and poly(ethylene glycol) (PEG) as a standard sample. The transmittance of the copolymer in phosphate buffered saline (PBS) (pH = 7.4, 0.1 wt/v%) was measured by UV-visible spectroscopy (JASCO International, Japan) with 1.0 °C/min of heating rate. The lower critical solution temperature (LCST) of the copolymer was defined as the temperature at 50% of transmittance.

Fabrication of Nanofibers: The poly(NIPAAm-*co*-HMAAm) solution was prepared by dissolving the copolymer in 1,1,1,3,3,3 hexafluoro-2-propanol (HFIP, 3 mL) (Sigma-Aldrich, USA) at 15 w/v%. The MNPs (Ferrotec, Japan, 0.1 or 0.2 g) and DOX (Sigma-Aldrich, USA, 1 mg) were dissolved in distilled water (300 μL). The copolymer and MNPs/DOX solutions were mixed in a 10/1 ratio to obtain 18–31 wt% and 0.18 wt% of the final weight fractions of MNPs and DOX in the polymer, respectively.[31] The solution was then electrospun into nanofibers at a constant flow rate (0.5 mL/h) with a gap between an aluminum foil-wrapped plate collector and a needle (23–25 gauge) of 19 cm at a driving DC voltage of 20 kV (Nanon-01A, MECC Co., Ltd., Japan). The residual solvent in all of electrospun nanofibers was removed in a pressure reduced vacuum oven. For crosslinking, the DOX/MNP-incorporated nanofiber composites were placed in an oven set with 130 °C for 12 h.

Characterization of Nanofibers: The morphologies of the crosslinked nanofibers were observed by scanning electron microscope (SEM, Hitachi, Japan) using secondary electrons (SE) and back-scattered electrons (BSE) signal types at an acceleration voltage of 10.0 and 20 kV, respectively. SEM images were taken after the samples were completely dried and ion-sputter coated with platinum (Pt) for 30 seconds using ion sputter (Hitachi, Japan). Transmission electron microscope (TEM, JEOL, Japan) was used for confirmation of the loaded MNPs in the nanofiber with an accelerating voltage of 10 kV. The TEM sample was prepared by directly electrospinning copolymers onto a copper grid and completely dried before observation. Atomic force microscope (AFM, Asylum Research, USA) was also used for observation of the morphologies of nanofibers under wet condition with micro cantilever (spring constant; 12 N/m, resonant frequency; 127 kHz, SII, Japan). Samples were first equilibrated in PBS at 20 or 50 °C and the fiber morphologies were examined after removing the excess water (scan size: 5.00 μm, scan rate: 0.02 Hz). To confirm the success of intermolecular crosslinking after thermal curing, the degree of self-condensation of the methylol groups of HMAAm was calculated from the disappearance of the methylol groups in nanofibers by ATR-FTIR spectroscopy (IRPrestige-21, Shimadzu, Japan). The number of reacted methylol groups was calculated from the calibration curve of absorbance at 1050 cm^{-1}.[1c] The weight percentages of MNPs in nanofibers were calculated from the weight loss of MNP-loaded nanofibers by thermogravimetric analysis (TGA, SII Nanotechnology, Japan). Sample was placed in an Al pan and heated at rate of 10 °C/min from 25 to 600 °C. The MNPs content was calculated from the weight loss of the organic compounds. The composition of the MNPs in the nanofiber was also determined by energy dispersive X-ray spectroscopy (EDX, equipped in SEM, Horiba, Japan). The crystal structure and the phase composition of the MNPs in the nanofibers were determined by X-ray diffraction (XRD, Riraku, Japan) between 10 and 80° with 5°/min of scan rate.

AMF-Induced Heat Generation Properties: The heat generation properties of the MNP-loaded nanofibers were investigated by applying

an alternating magnetic field (AMF, HOTSHOT2, Ameritherm, USA).[32] Approximately 5, 15 and 25 mg of the DOX/MNPs-nanofibers were immersed in PBS (300 μL) at 4 °C and swollen for 10 min. The sample was placed in a copper coil (ten turns with inside and outside diameters of 5 and 6 cm, respectively). Heating was induced by the AMF generated by passing alternating current (480 A, 166 kHz frequency, 362 W power) through the coil (Ameritherm, USA). The temperature profile of the suspension was monitored using a thermometer (As One, Japan). The infrared thermal images of the heated fibers were also obtained from 2D infrared thermometer camera (Tech-Jam, Japan).

Equilibrium Swelling Ratio: The dried DOX/MNPs-nanofibers were immersed in PBS (1 mL) at 25 °C and equilibrated for 10 min. The sample was first placed in a copper coil. The AMF was turned 'on' for 300 s allowing the fibers to heat to 45 °C. The AMF was then turned 'off' allowing cooling down to 25 °C. This process was repeated for 4 times. The swelling ratio was calculated using the following equation;

$$Swelling\ ratio = (W_{swell} - W_{dry})/W_{dry} \quad (1)$$

where W_{swell} and W_{dry} are the weights of the swollen and dry DOX/MNPs-nanofibers, respectively.

DOX Release Test: The dried DOX/MNPs-nanofibers were immersed in 1 mL of PBS at 25 °C and equilibrated for 10 min. The sample was first placed in a copper coil. The AMF was turned 'on' for 300 s allowing the fibers to heat to 45 °C. The AMF was then turned 'off' allowing cooling down to 25 °C. This process was repeated for 4 times. The released DOX during each cycle was collected and its absorbance at 480 nm was measured by UV-visible spectroscopy (JASCO International, Japan). The cumulated released DOX was calculated using the following equation;

$$Cumulated\ released\ DOX = D_{released\ at\ X}/D_{total} \times 100(\%) \quad (2)$$

where $D_{released\ at\ X}$ is the cumulative amounts of released DOX at X cycle of AMF alternation and D_{total} is the total amounts of incorporated DOX in the nanofibers.

According to the Equation 2 and drug release data Figure 4, approximately 45% (approximately 13 μg/mL) of the loaded DOX were released upon AMF application. In the further cytotoxicity study, therefore, we set the dose of free DOX 10 μg/mL, which is enough to kill cancer cells *in vitro* according to the previous report.[33]

In Vitro Hyperthermia Study: A cytotoxicity study of all nanofibers was evaluated using human melanoma cell line COLO 679 cells (RIKEN cell bank, Japan). The cells were cultured on 24-well tissue culture polystyrene dish (TCPS, Falcon, USA) with cell culture media including RPMI 1640 (Gibco, USA), 20% of fetal bovine serum (FBS, MP Biomedicals, USA), and 1% of penicillin streptomycin (P/S, Gibco, USA). The cells (1.0×10^4 cells/well) were cultured in a 37 °C incubator with 5% CO_2 atmosphere for 2 days. MNPs-nanofiber or DOX/MNPs-nanofiber was then added to the medium and cells were co-incubated with the nanofibers at 37 °C for another 24 h. On testing the hyperthermia effect on the cells, an AMF was turned 'on' at day 3 for approximately 5 min until the medium temperature reached at 45 °C. The temperature was maintained for 5 min and the AMF was then turned 'off' allowing cooling down to 37 °C. This treatment was repeated again at day 4. Cells were also incubated in the absence of nanofibers with and without free DOX addition (10 μg/mL) at day 3 and day 4. The cytotoxicity was evaluated by 3-(4, 5-dimethylthiazolyl-2)-2,5-diphenyltetrazolium bromide assay (MTT assay, BioAssay System, USA) at 1, 3, 4 and 5 days of cultivation. Cells were treated with MTT solution (50 μL) for 4 h and then incubated with detergent reagent (500 μL) for 2 h. The supernatants were placed 96-well micro plate and the absorbance at 570 nm was measured by ELISA micro-plate reader (BIO-RAD Laboratories). The proliferation index was defined as the ratio of the cell numbers on day D to that on day 1 as follow;

$$Proliferation\ index = N_D/N_{D=1} \quad (3)$$

where N_D and $N_{D=1}$ are cell numbers on day D and day 1, respectively.

The viability of the cells was also demonstrated by fluorescent staining with annexin V Cy-3 (BioVision, USA) and terminal deoxynucleotidyl transferase-mediated dUTP nick end labelling (TUNEL assay, Takara, Japan) assay. The cells were fixed in 4% para-formaldehyde at day 4 and day 5 for 15 min and the staining was carried out. Nuclei were also stained by the fluorescent dye DAPI (Sigma-Aldrich, USA). Staining was visualized using fluorescence microscope (IX71, Olympus).

Supporting Information

Supporting Information is available from the Wiley Online Library or from the author.

Acknowledgements

The authors would like to express their gratitude to the Grants-in-Aid for Young Scientists (A) (10013481) from the Ministry of Education, Culture, Sports, Science and Technology (MEXT) Japan. The authors are grateful to Prof. Allan S. Hoffman (University of Washington) and Dr. John M. Hoffman (Stratos Genomics Inc. in USA) for continued and valuable discussion.

Received: February 28, 2013
Revised: April 12, 2013
Published online: June 14, 2013

[1] a) H. Okuzaki, K. Kobayashi, H. Yan, *Synth. Met.* **2009**, *159*, 2273; b) G. D. Fu, L. Q. Xu, F. Yao, K. Zhang, X. F. Wang, M. F. Zhu, S. Z. Nie, *Appl. Mater. Interfaces* **2009**, *1*, 239; c) Y.-J. Kim, M. Ebara, T. Aoyagi, *Sci. Technol. Adv. Mater.* **2012**, *13*, 064203; d) Y.-J. Kim, M. Ebara, T. Aoyagi, *Angew. Chem. Int. Ed.* **2012**, *51*, 10537; e) F. D. Benedetto, E. Mele, A. Camposeo, A. Athanassiou, R. Cingolani, D. Pisignano, *Adv. Mater.* **2008**, *20*, 314.

[2] a) S. Ramakrishna, K. Fujihara, W.-E. Teo, T. Yong, Z. Ma, R. Ramaseshan, *Mater. Today* **2006**, *9*, 40; b) S. Agarwal, J. H. Wendorff, A. Greiner, *Adv. Mater.* **2009**, *21*, 3343.

[3] a) M. Inagaki, Y. Yang, F. Kang, *Adv. Mater.* **2012**, *24*, 2547; b) V. Beachley, X. Wen, *Prog. Polym. Sci.* **2010**, *35*, 868.

[4] a) R. Uppal, G. N. Ramaswamy, C. Arnold, R. Goodband, Y. Wang, *J. Biomed. Mater. Res., Part B* **2011**, *97*, 20; b) P. Zahedi, I. Rezaeian, S.-O. R.-Siadat, S.-H. Jafari, P. Supaphol, *Polym. Adv. Technol.* **2010**, *21*, 77.

[5] a) S. Liu, J. Zhao, H. Ruan, T. Tang, G. Liu, D. Yu, W. Cui, C. Fan, *Biomacromolecules* **2012**, *13*, 3611; b) X. Zong, S. Li, E. Chen, B. Garlick, K.-S. Kim, D. Fang, J. Chiu, T. Zimmerman, C. Brathwaite, B. S. Hsiao, B. Chu, *Ann. Surg.* **2004**, *240*, 910.

[6] a) Z. Ding, R. B. Fong, C. J. Long, P. S. Stayton, A. S. Hoffman, *Nature* **2001**, *411*, 59; b) T. Miyata, N. Asami, T. Uragami, *Nature* **1999**, *399*, 766; c) M. Ebara, M. Yamato, T. Aoyagi, A. Kikuchi, K. Sakai, T. Okano, *Adv. Mater.* **2008**, *20*, 3034; d) M. Ebara, K. Uto, N. Idota, J. M. Hoffman, T. Aoyagi, *Adv. Mater.* **2012**, *24*, 273; e) M. Ebara, J. M. Hoffman, A. S. Hoffman, P. S. Stayton, *Adv. Mater.* **2006**, *6*, 843.

[7] a) J. J. Lai, J. M. Hoffman, M. Ebara, A. S. Hoffman, C. Estournes, A. Wattiaux, P. S. Stayton, *Langmuir* **2007**, *23*, 7385; b) D. Shi, *Adv. Funct. Mater.* **2009**, *19*, 3356; c) Y.-W. Jun, J.-H. Lee, J. Cheon, *Angew. Chem. Int. Ed.* **2008**, *47*, 5122; d) O. Veiseh, J. W. Gunn, M. Zhang, *Adv. Drug Delivery Rev.* **2010**, *62*, 284; e) Y. Li, G. Huang, X. Zhang, B. Li, Y. Chen, T. Lu, T. J. Lu, F. Xu, *Adv. Funct. Mater.* **2013**, *23*, 660; f) C. M.-Boubeta, K. Simeonidis, D. Serantes, I. C.-Leboran, I. Kazakis, G. Stefanou, L. Pena, R. Galceran, L. Balcells, C. Monty, D. Baldomir, M. Mitrakas, M. Angelakeris, *Adv. Funct. Mater.* **2012**, *22*, 3737.

[8] a) T.-C. Lin, F.-H. Lin, J.-C. Lin, *Acta Biomater.* **2012**, *8*, 2704; b) R. Hergt, S. Dutz, R. Muller, M. Zeisberger, *J. Phys.: Condens.*

Matter **2006**, *18*, S2919; c) S. Mornet, S. Vasseur, F. Grasset, E. Duguet, *J. Mater. Chem.* **2004**, *14*, 2161; d) D. Yoo, H. Jeong, C. Preihs, J.-S. Choi, T.-H. Shin, J. L. Sessler, J. Cheon, *Angew. Chem. Intl. Ed.* **2012**, *51*, 12377; e) B. Mehdaoui, A. Meffre, J. Carrey, S. Lachaize, L.-M. Lacroix, M. Gougeon, B. Chaudret, M. Respaun, *Adv. Funct. Mater.* **2011**, *21*, 4573.

[9] a) A. Y. Cheung, A. Neyzari, *Cancer Res.* **1984**, *44*, 4736s; b) T. Tagami, M. J. Ernsting, S.-D. Li, *J. Controlled Release* **2011**, *152*, 303.

[10] C. D. Kowal, J. R. Bertino, *Cancer Res.* **1979**, *39*, 2285.

[11] a) W. Xiong, W. Wang, Y. Wang, Y. Zhao, H. Chen, H. Xu, X. Yang, *Colloids Surf., B* **2011**, *84*, 447; b) Z. S. A.-Ahmady, W. T. A.-Jamal, J. V. Bossche, T. T. Bui, A. F. Drake, A. J. Mason, K. Kostarelos, *ACS Nano* **2012**, *6*, 9335; c) W. T. Al-Jamal, Z. S. Al-Almady, K. Kostarelos, *Biomaterials* **2012**, *33*, 4608; d) S. J. Lee, M. Muthiah, H. J. Lee, H.-J. Lee, M.-J. Moon, H.-L. Che, S. U. Heo, H.-C. Lee, Y. Y. Jeong, I.-K. Park, *Macromol. Res.* **2012**, *20*, 188.

[12] a) S. M. Hussain, K. L. Hess, J. M. Gearhart, K. T. Geiss, J. J. Schlager, *Toxicol. In Vitro* **2005**, *19*, 975; b) B. Ankamwar, T. C. Lai, J. H. Huang, R. S. Liu, M. Hsiao, C. H. Chen, Y. K. Hwu, *Nanotechnology* **2010**, *21*, 075102; c) N. Sadghiani, L. S. Barbosa, L. P. Silva, R. B. Azevedo, P. C. Morais, Z. G. M. Lacava, *J. Magn. Magn. Mater.* **2005**, *289*, 466; d) N. Singh, G. J. S. Jenkins, R. Asadi, S. H. Doak, *Nano Rev.* **2010**, *1*, 5358.

[13] A. L. Yarin, W. Kataphinan, D. H. Reneker, *J. Appl. Phys.* **2005**, *98*, 064501.

[14] N. Bhattarai, M. Zhang, *Nanotechnology* **2007**, *18*, 455601.

[15] H. Okuzaki, K. Kobayashi, H. Yan, *Macromolecules* **2009**, *42*, 5916.

[16] N. Bhardwaj, S. C. Kundu, *Biotechnol. Adv.* **2010**, *28*, 325.

[17] J. Shawon, C. Sung, *J. Mater. Sci.* **2004**, *39*, 4605.

[18] a) K. Kanjanapongkul, S. Wongsasulak, T. Yoovidhya, *J. Appl. Polym. Sci.* **2010**, *118*, 1821; b) D. G. Yu, X. Wang, X. Y. Li, W. Chen, Y. Z. Liao, *Acta Biomater.* **2013**, *9*, 5665; c) J. S. Jeong, S. Y. Jeon, T. Y. Lee, J. H. Park, J. S. Shin, P. S. Alegaonkar, A. S. Berdinsky, J. B. Yoo, *Diam. Relat. Mater.* **2006**, *15*, 1839; d) D. Shi, J. Lian, P. He, L. M. Wang, F. Xiao, L. Yang, M. J. Schulz, D. B. Mast, *Appl. Phys. Lett.* **2003**, *83*, 5301.

[19] a) A.-H. Lu, E. L. Salabas, F. Schuth, *Angew. Chem. Intl. Ed.* **2007**, *46*, 1222; b) S. Laurent, D. Forge, M. Port, A. Roch, C. Robic, L. V. Elst, R. N. Muller, *Chem. Rev.* **2008**, *108*, 2064.

[20] a) L. Jeong, K. Y. Lee, W. H. Park, *Key Eng. Mater.* **2007**, *342*, 813; b) Y. Su, C. H. He, Y. F. Qian, X. Q. Li, H. S. Wang, *Iran Polym. J.* **2010**, *19*, 123.

[21] J. Carrey, B. Mehdaoui, M. Respaud, *J. Appl. Phys.* **2011**, *109*, 083921.

[22] a) K. Kendall, M. R. Kosseva, *Colloids Surf., A* **2006**, *286*, 112; b) C. F. Hayes, *J. Colloid Interface Sci.* **1975**, *52*, 239.

[23] a) C. S. S. R. Kumar, F. Mohammad, *Adv. Drug Delivery Rev.* **2011**, *63*, 789; b) K. H. Polderman, I. Herold, *Crit. Care Med.* **2009**, *37*, 1101.

[24] a) Y. Kaneko, S. Nakamura, K. Sakai, T. Aoyagi, A. Kikuchi, Y. Sakurai, T. Okano, *Macromolecules* **1998**, *31*, 6099; b) J. Wang, A. Sutti, X. Wang, T. Lin, *Soft Matter* **2011**, *7*, 4364; c) M. M. Ozmen, M. V. Dinu, E. S. Dragan, O. Okay, *J. Macromol. Sci., Pure Appl. Chem.* **2007**, *44*, 1195.

[25] J. Yang, C.-H. Lee, H.-J. Ko, J.-S. Suh, H.-G. Yoon, K. Lee, Y.-M. Muh, S. Haam, *Angew. Chem. Int. Ed.* **2007**, *46*, 8836.

[26] a) S. Wang, E. A. Konorev, S. Kotamraju, J. Joseph, S. Kalivendi, B. Kalyanaraman, *J. Biol. Chem.* **2004**, *279*, 25535; b) R. Kumari, A. Sharma, A. K. Ajay, M. K. Bhat, *Mol. Cancer* **2009**, *8*, 87; c) M. V. Fiandalo, N. Kyprianou, *Exp. Oncol.* **2012**, *34*, 165.

[27] a) S. Brule, M. Levy, C. Wilhelm, D. Letourneur, F. Gazeau, C. Menager, C. L. Visage, *Adv. Mater.* **2011**, *23*, 787; b) J. R. McDaniel, S. R. MacEwan, M. Dewhirst, A. Chikoti, *J. Controlled Release* **2012**, *159*, 362; c) L. Li, T. L. M. T. Hagen, D. Schipper, T. M. Wijnberg, G. C. van Rhoon, A. M. M. Eggermont, L. H. Lindner, G. A. Koning, *J. Controlled Release* **2010**, *143*, 274.

[28] a) H. Okada, T. W. Mak, *Nat. Rev. Cancer* **2004**, *4*, 592; b) J. Max, *Science* **1993**, *259*, 760–761; c) G. T. Williams, *Cell* **1991**, *65*, 1097.

[29] S.-L. Weng, S. L. Taylor, M. Morshedi, A. Schuffner, E. H. Dura, S. Beebe, S. Oehninger, *Mol. Hum. Reprod.* **2002**, *8*, 984.

[30] R. H. Yocum, E. B. Nyquist, *Functional Monomers*, *Vol. 1*, Marcel Dekker Inc., New York **1973**.

[31] a) J. T. Kannarkat, J. Battogtokh, J. Philip, O. C. Wilson, P. M. Mehl, *J. Appl. Phys.* **2010**, *107*, 09B307; b) H. Hu, W. Jiang, F. Lan, X. Zenh, S. Ma, Y. Wu, Z. Gu, *RSC Adv.* **2013**, *3*, 879; c) X. Xu, L. Yang, X. Xu, X. Wang, X. Chen, Q. Liang, J. Zeng, X. Jing, *J. Controlled Release* **2005**, *108*, 33; d) J. Zeng, L. Yang, Q. Liang, X. Zhang, H. Guan, X. Xu, X. Chen, X. Jing, *J. Controlled Release* **2005**, *105*, 43.

[32] P. Techawanitchai, K. Yamamoto, M. Ebara, T. Aoyagi, *Sci. Technol. Adv. Mater.* **2011**, *12*, 044609.

[33] a) J. Woodley-Cook, L. Y. Y. Shin, L. Swystun, S. Caruso, S. Beaudin, P. C. Liaw, *Mol. Cancer Ther.* **2006**, *5*, 3303; b) S. S. Park, Y.-W. Eom, K. S. Choi, *Biochem. Biophys. Res. Commun.* **2005**, *334*, 1014; c) J.-J. Lee, B. C. Kim, M.-J. Park, Y.-S. Lee, Y.-N. Kim, B. L. Lee, J.-S. Lee, *Cell Death Differ.* **2011**, *18*, 666.